JOURNAL OF THE MECHANICAL BEHAVIOR OF BIOMEDICAL MATERIALS 30 (2014) 103–110

Available online at www.sciencedirect.com

ScienceDirect

www.elsevier.com/locate/jmbbm

Research Paper

Mechanical and thermal properties of hot pressed CoCrMo–porcelain composites developed for prosthetic dentistry

B. Henriques[a,c,*], M. Gasik[b], J.C.M. Souza[a], R.M. Nascimento[c], D. Soares[a], F.S. Silva[a]

[a]Center for Mechanical and Materials Technologies, Universidade do Minho, Campus de Azurém, 4800-058 Guimarães, Portugal

[b]Department of Materials Science and Engineering, School of Chemical Technology, Aalto University Foundation, 00076 Aalto, Espoo, Finland

[c]Departamento de Engenharia de Materiais, Universidade Federal do Rio Grande do Norte (UFRN), 59072-970 Natal/RN, Brazil

ARTICLE INFO

Article history:
Received 3 June 2013
Accepted 21 October 2013
Available online 7 November 2013

Keywords:
CoCrMo alloy
Porcelain
Composite
Powder metallurgy
Mechanical properties
Thermal properties

ABSTRACT

In this study, mechanical and thermal properties of CoCrMo–porcelain composites for dental restorations have been evaluated. These metal–ceramic composites were produced by powder metallurgy and hot pressing techniques from the mixtures of metal and ceramic powders with different volume fractions. Young's moduli and the coefficient of thermal expansion of materials were evaluated by dynamic mechanical analysis (DMA) and dilatometry (DIL) tests, respectively. The strength in flexion and shear was measured with a universal test machine and hardness with a respective tester. The microstructures and fracture surfaces were inspected by the means of optical microscopy and Scanning Electron Microscopy/Energy Dispersive Spectroscopy (SEM/EDS).

Shear strength, Flexural strength and Young' moduli of ceramic and metal-matrix composites were found to increase with higher metal particles content. The DMA tests performed at different frequencies showed no frequency-dependent features of the materials studied, indicating no viscoelastic behavior. The fracture surfaces analysis suggests the load-transfer mechanism be possibly responsible for this behavior, as the differences in CTE are low enough to cause significant thermal stresses in these materials. The results might be included in a materials properties database for further use for design and optimization of dental restorations.

1. Introduction

Dental restorations such crowns and fixed partial dentures (FPDs) are designed to restore functionality and esthetics to failed teeth. The failures of aforementioned restorative systems are undesired occurrences as they often imply money expenditure and discomfort to patients. The main causes to which dental restorative systems failures are attributed are:

*Corresponding author at: Center for Mechanical and Materials Technologies, University of Minho, Campus de Azurém, 4800-058 Guimarães, Portugal. Tel.: +35 1253510220; fax: +35 1253516007.
E-mail address: brunohenriques@dem.uminho.pt (B. Henriques).

1751-6161/$ - see front matter © 2013 Elsevier Ltd. All rights reserved.
http://dx.doi.org/10.1016/j.jmbbm.2013.10.023

the incorrect selection of materials; the incorrect processing of materials; the incorrect design of the component; the presence of defects (e.g. cracks and pores) in the prostheses, either in the veneering porcelain or in the substructure; and the interfacial breakdown of the bond between the veneering porcelain and the substructure (metal or ceramic) (Yesil et al., 2009; Özcan, 2003; Anusavice, 2012; Swain, 2009). Several studies have been addressed to this topic and new solutions and approaches have been proposed in order to strengthen the restorative base materials (mainly the porcelain) and, more importantly, the bond between them (Anusavice et al., 1977a, 1977b; Maira and Padipatvuthikulb, 2010; Carrado and Palkowski, 2010; Özcan and Uysal, 2005; Bieniaś et al., 2009). The bond strength between porcelain and metallic substrates have been reported to increase for the following situations: the addition of easy-oxide forming elements to noble alloys (Hautaniemi, 1995); the coating of reactive metals surfaces (e.g. titanium alloys and CoCrMo alloys) with oxide-controlling elements (Özcan and Uysal, 2005; Bieniaś et al., 2009; Elsaka et al., 2010); the use of bonding agents (Yesil et al., 2009; Wagner et al., 1993), among others.

More recently, alternative methods based on Functionally Graded Materials (FGMs) philosophy have been proposed aiming the enhancement the overall performance of metal–ceramic and all-ceramic dental restorative systems. Graded dental restorations have been shown to display improved features relative to conventional ones, namely higher resistance to contact and sliding (Suresh, 2001); higher adhesion of porcelain to the substructure (metal or ceramic) (Henriques et al., 2011; Henriques et al., 2012a, 2012b; Zhang and Kim, 2009); improved aesthetical properties and improved behavior under fatigue conditions (Henriques et al., 2012b). The rising trend to apply composite materials (including FGMs) in biomedical components, in general, and in restorative dentistry, in particular, have raised the need for creating composites properties databases that allow scientists and engineers to make use of them in the design process of new components. These databases may be particularly useful in designing FGM structures using Finite Element Methods (FEMs). Because FGMs encompasses gradients at one or several levels (macro-, micro- and nano-scale), they are not described by the same models and approximations used for traditional composites. Therefore, FEMs became the most suited and used tool for FGM modeling and analysis (Gasik, 1998). A good example could be the determination of the stresses state at the interfacial region of a graded metal–ceramic dental restoration by FEM, after cooling from porcelain sintering and also upon occlusal loading. The out coming results are expected to be more consistent with reality if the materials properties data used in the FEM study had been obtained experimentally. Therefore, this study focused on the assessment of the mechanical properties of CoCrMo–porcelain composites for restorative dentistry applications, namely Young's modulus, transverse rupture strength and shear strength. The microstructure and fracture surface of composite materials were also analyzed.

2. Materials and methods

2.1. Materials

In this study a CoCrMo alloy (Nobil 4000, Nobilmetal, Villafranca d'Asti, Italy) and a dental porcelain (Ceramco3, Dentsply, York, USA) (Batch no. 08004925) were used. The chemical compositions of the metallic and ceramic particles are presented in Tables 1 and 2, respectively. The micrographs of CoCrMo and porcelain particles are shown in Fig. 1. The CoCrMo particles display spherical shape and a broad size distribution: D_{10}=4.44 μm; D_{50}=8.27 μm and D_{90}=12.76 μm.

2.2. Processing

The manufacturing of the metal–ceramic composite specimens comprised the following steps: several powder mixtures with different metal/porcelain volume fractions were produced. After weighting, the powders mixtures were blended in a rotary machine at 40 rpm during 10 min. The following mixtures were produced (vol%): pure porcelain (with 0% metal) and compositions with 20% metal, 40%, 60%, 80% and 100% metal, marked further as "*nn*M" where *nn* stays for the percentage of metal phase. Afterwards, the powder mixtures were hot pressed in a graphite die (Fig. 2). The hot pressing sequence comprised the following steps: first, the cavity of the graphite die was veneered with ZrO_2 paint to prevent carbon diffusion to specimens. Then the metal–ceramic powder mixture was inserted into the cavity. The hot pressing was performed under vacuum ($\sim 10^{-2}$ mBar) at a temperature of 970 °C and a constant pressure of ~20 MPa. The selected heat rate was 70 °C/min and after a 2 min stage at 970 °C the induction heating furnace was shut down.

Two types of specimen geometries were processed, rectangular and cylindrical. The dimensions of the rectangular samples used for flexural tests were $36 \times 6 \times 2.5$ mm^3, while those of the cylindrical samples used for shear tests were ⌀4×4 mm.

2.3. Mechanical tests

The composites and the monolithic base materials were subjected to shear tests and to three-point flexural tests to in order to assess the shear strength and the transverse strength, respectively.

Young's moduli measurements of all materials were obtained by the means of Dynamic Mechanical Analysis (DMA 242 C, Netzsch Gerätebau GmbH, Germany) using a

Table 1 – Base alloy composition (wt%) (according to manufacturer).

Co	Cr	Mo	Si	Traces
62	31	4	2.2	Mn, Fe, W

Table 2 – Porcelain chemical composition (wt%).

SiO_2	Al_2O_3	K_2O	SnO_2	ZrO_2	CaO	P_2O_5	Na_2O	Other traces
41.3	14.5	14.0	11.9	5.8	4.1	4.1	3.0	MgO, SO_3, ZnO, Cr_2O_3, Fe_2O_3, CuO, Rb_2O

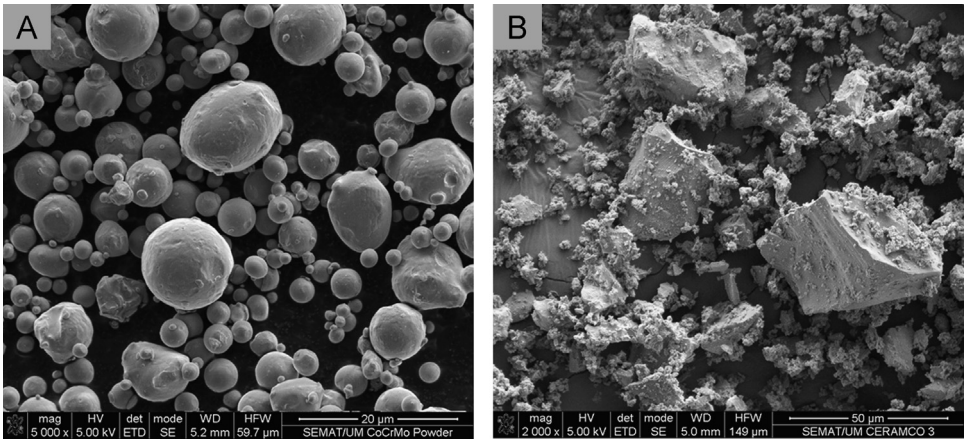

Fig. 1 – Micrograph of the metal and ceramic powders: (A) CoCrMo particles and (B) porcelain powders.

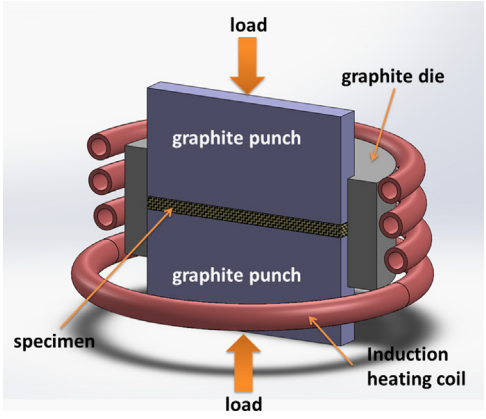

Fig. 2 – Hot pressing schematic. Specimen is pressed between the two graphite punches at high temperatures.

three-point bending sample holder. The coefficient of thermal expansion (CTE) of composites and the monolithic materials was also assessed using dilatometry (DIL 402C, Netzsch Gerätebau GmbH, Germany).

The shear bond strength tests were carried out at room temperature and performed in a universal testing machine (Instron 8874, MA, USA), with a load cell of 25 kN capacity and under a crosshead speed of 0.5 mm/s. Tests were performed in a custom-made stainless steel apparatus (Fig. 2) similar to that described by Henriques et al. (2011). The apparatus consisted in two sliding parts A and B, each one with a hole perfectly aligned to the other. After aligning the holes, the specimens were inserted and loaded in the interface in the interface until fracture. The shear bond strength (MPa) was calculated by the dividing the highest recorded load (N) by the cross sectional area of resistant porcelain (mm^2).

Transverse rupture strength (TRS) was calculated as follows:

$$\sigma_{TRS} = \frac{3FL}{2bh^2}$$

where, σ_{TRS} is the transverse rupture strength of the specimen (MPa), F is the force required to rupture the specimen (N), L is the length of specimen span relative to fixture (35 mm), b is the width of the specimen (mm) and h is the thickness of specimen (mm) (Fig. 3A). Shear strength was calculated as follows:

$$\tau_{SS} = \frac{F}{hD}$$

where τ_{SS} is the shear strength (MPa), F is the force to rupture (N), h is the height of the specimens (mm), and D is the diameter of the specimens (mm) (Fig. 3B).

The hardness evaluation was also performed using a microhardness tester (DuraScan 20, Emcotest, Kuchl, Austria). Five indentations with 1000g load during 15 s were made in each sample and the mean value and standard deviation was calculated afterwards.

2.4. *Analysis of the metal–porcelain interface and failure mode*

The representative fracture surfaces of the tested composites were evaluated by optical microscopy (Axiotech, Carl Zeiss, USA) and SEM/EDS (Nova 200, FEI, OR, USA). For microstructure analysis, the specimens were embedded in auto-polymerizing resin, ground finished to 1200-grit SiC paper and polished with diamond paste first in 6 µm and finally in 1 µm felt disc.

3. Results and discussion

3.1. Microstructure

Fig. 4 shows the micrographs of the monolithic materials (A – porcelain ,0 M and F – CoCrMo alloy, 100 M) and metal–ceramic composites (B – 20 M; C – 40 M; D – 60 M; and E – 80 M). The micrographs revealed flawless microstructures, with no pores or cracks being detected at a significant level.

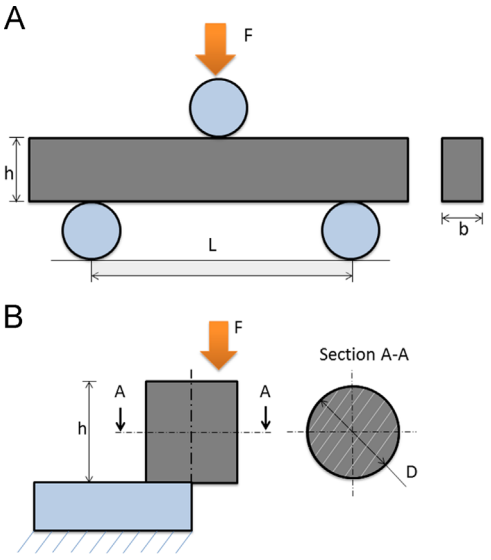

Fig. 3 – Schematic of the test configurations used to determine the mechanical properties of the metal/ceramic composites. (A) Three-point bending flexural test and (B) shear strength test.

A good distribution of the metallic particles in the ceramic matrix (20 M and 40 M) and ceramic particles in the metallic matrix (60 M and 80 M) could be observed. From micrographs shown in Fig. 4C and D, corresponding to compositions of 40 M and 60 M, changes in percolation level could be noticed reflected in different interconnecting networks of ceramic and metallic phases, respectively. These metal–ceramics composites configurations can be defined as co-continuous metal–ceramic composites (Agrawal and Sun, 2004). The composites micrographs also indicate a good adhesion between metallic and ceramic particles as no particles pull-outs were observed during the samples polishing.

3.2. Mechanical properties

Figs. 5 and 6 show the load–displacement curves for the monolithic and metal–ceramic composites obtained in the shear and flexural tests, respectively. In Table 3 the experimental results obtained for coefficient of thermal expansion (CTE), hardness (HV1), Young's modulus (YM), shear strength (SS) and flexural strength (FS) are summarized.

The results show an increase in the SS, FS and YM of the ceramic matrix composites with increasing metallic particles content (20 M and 40 M). This improvement in mechanical properties is in accordance with findings reported elsewhere involving MMC reinforced with glass-based ceramics (Oksiuta et al., 2009). Shear strength increased approximately 80% for both 20 M and 40 M composites. The similar increasing trend was observed in the flexural strength, by 60% and 100%, for 20 M and 40 M, respectively. It must be noted the drop of the strength for 100 M specimen (Fig. 6) is due shorter hot pressing time (10 min only) vs. other parameters of these samples. Complementary tests (not plotted in Fig. 6 but

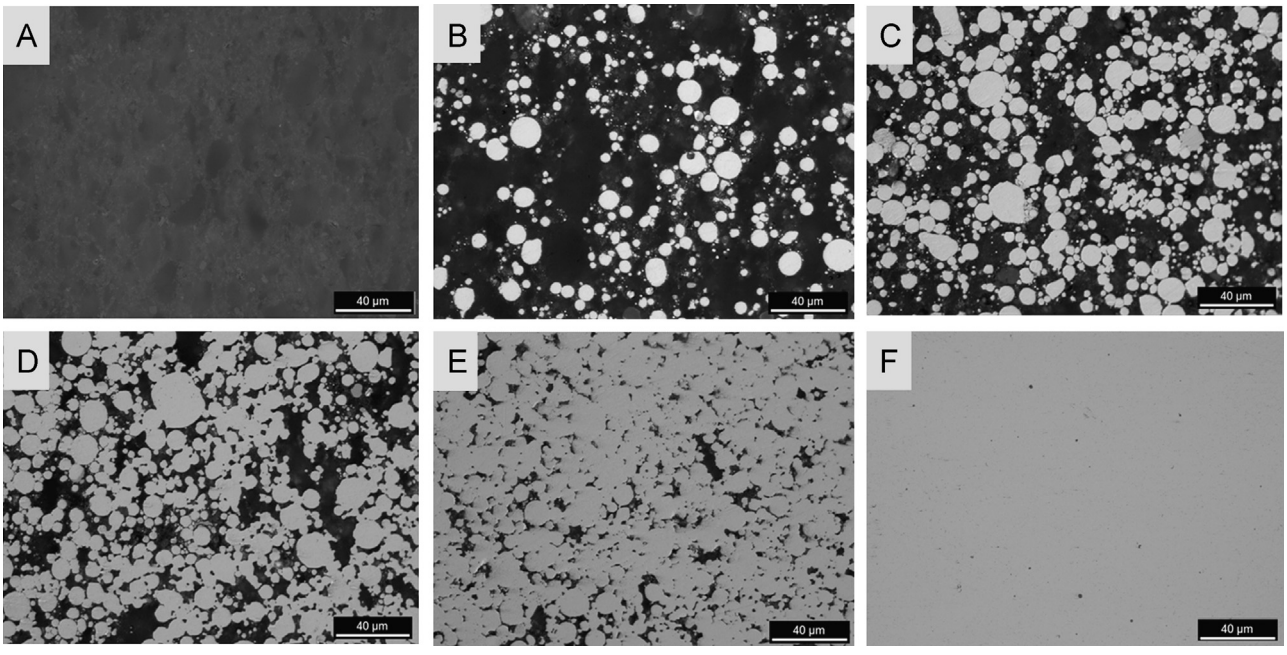

Fig. 4 – Micrographs of the metal/ceramic composites with different metal (M) contents: (A) 0 M, (B) 20 M, (C) 40 M, (D) 60 M, (E) 80 M, and (F) 100 M.

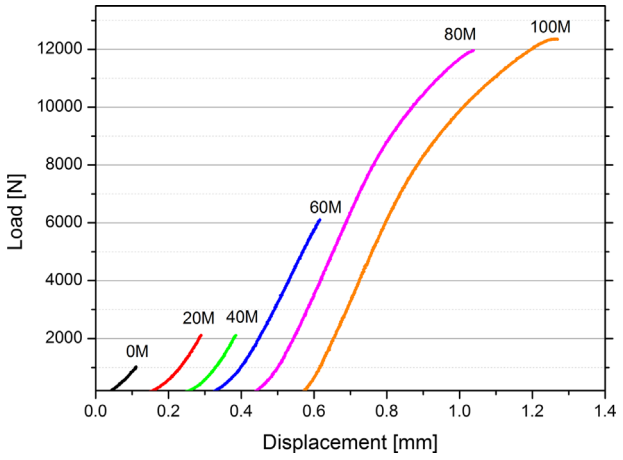

Fig. 5 – Plot of the load–displacement curves obtained in the shear test of metal–ceramic composites and monolithic base materials. The curves have been shifted horizontally to improve readability.

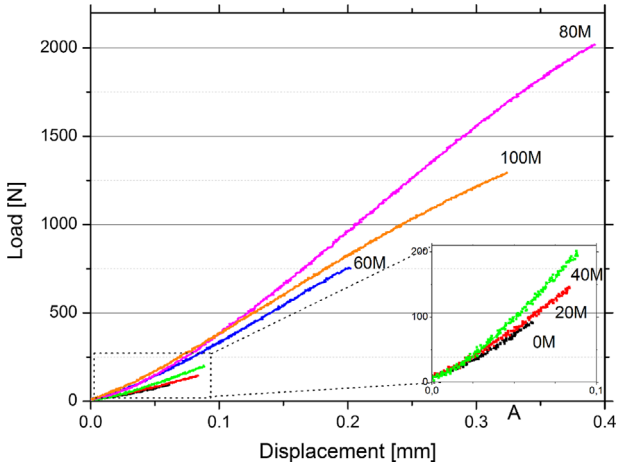

Fig. 6 – Plot of the load–displacement curves obtained in the flexural strength test of metal–ceramic composites and monolithic base materials.

shown in Table 3) confirmed higher flexural strengths for longer hot pressing times.

The increase in YM, SS and FS confirms that a good bonding between the two phases of the composites was achieved and suggests that a load-transfer mechanism can be active. This load-transfer mechanism is the strengthening mechanism that has been proposed for composites without substantial thermal expansion mismatch and with a strong interfacial bonding (Dlouhy and Boccaccini, 1996). The coefficient of thermal expansion (CTE) of metal–ceramic composites is often assumed to take intermediate values between that of metal and of ceramics. However, the present CTE data did not fit within simplified Voigt or Reuss models of rules of mixtures (Gasik, 1998), despite that the addition of metallic phase to the porcelain clearly shown increase of the CTE of the composite. Similar results were reported for CoCrMo based composites reinforced with bioactive glass (Oksiuta et al., 2009). These two conditions are verified in the present study as the CTE mismatch between metal and porcelain is not high, compared to those values reported elsewhere (Agrawal and Sun, 2004), and the bond strength between metal and porcelain was shown to be high (Henriques et al., 2012c, 2012d, 2013). Residual thermal stresses due to CTE mismatch in metal and ceramic phases were demonstrated to affect the failure mechanisms inside the composites (Agrawal and Sun, 2004).

The strengthening mechanisms provided by the metallic particles in CMCs can be further explained by the higher elastic modulus of the reinforcement phase (metallic particles) relative to that of the matrix (porcelain). The incorporation of a ductile, metallic, secondary phase in glass and glass-ceramics matrix has been shown to improve mechanical properties and fracture toughness (Dlouhy and Boccaccini, 1996).

The metal-matrix composites (60 M and 80 M) displayed an increase in the SS and YM with decreasing ceramic particles content. For 30 min hot pressing time for 100 M specimen ductile behavior was also observed vs. more fragile behavior for the 100 M specimen hot pressed for 10 min only (Figs. 5 and 6). Similarly to 100 M specimen (with 10 min hot pressing time), all others exhibited fragile behavior, with no plastic deformation being observed in the flexural

Table 3 – Mechanical and thermal properties of the CoCrMo–porcelain composite materials obtained experimentally by powder metallurgy and hot pressing techniques.

	CTE [1/10^{-6}]	Hardness [HV1]	E [GPa]	Shear tests		3-Point-bending tests	
				Rupture load [N]	Rupture strength [MPa]	Rupture load [N]	TRS [MPa]
0 M	8.6	596±8	52	1020	83	92	57
20 M	8.7	542±19	63	2120	151	146	93
40 M	11.0	513±14	89	2106	147	202	122
60 M	11.6	484±12	145	6111	437	753	480
80 M	12.1	429±24	200	11960	871	2019	1187
100 M	12.9	427±5	170/ 220*	12350	965	1296/ 1773*	732.9/ 2616*

Results marked with asterisk (*) correspond to 100 M samples hot pressed during 30 min. The other 100 M samples were hot pressed during 10 min. Hardness of hot pressed CoCrMo (100 M) is higher than that reported for the cast CoCrMo alloy (Henriques et al., 2012d).

load–displacement curves (Fig. 5) or revealed by the fractography analysis presented below. Concerning the mechanical behavior of MMCs exhibited in this study, the ceramic phase (porcelain) had lower yield strength and lower Young's modulus than the metallic matrix (CoCrMo). Therefore, the ceramic phase was most likely acting as pores or defects in the matrix rather than as reinforcing elements. This fact can explain the drop in mechanical properties (SS, FS and YM) of these composites for increasing ceramic contents.

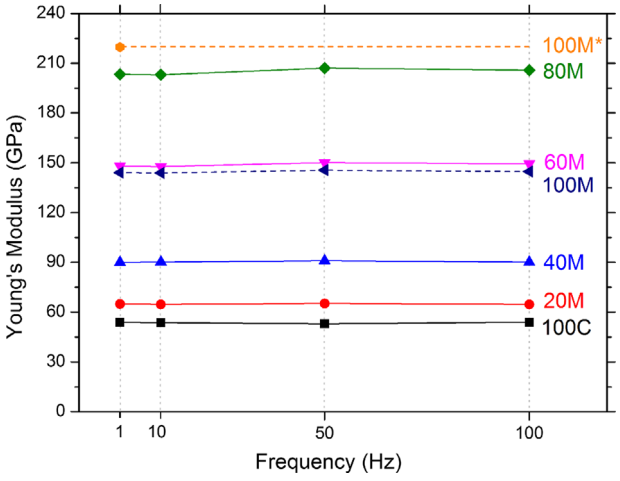

Fig. 7 – Young's modulus vs. loading frequencies of the metal/ceramic composites and monolithic materials. 100 M* corresponds to CoCrMo samples hot pressed at 1000 °C for 30 min.

Fig. 7 shows a plot of Young's moduli vs. DMA testing frequency for the monolithic and composite materials. Young's moduli of all materials show no frequency-dependent behavior, i.e., no evident viscoelastic behavior could be observed among them at room temperature. Testing the materials' elastic behavior at different frequencies was intended to simulate the clinical conditions, as different testing frequencies would simulate the different strain rates occurring on materials at the chewing and biting actions. Thus, a soft bite would result in a small strain rate being imposed to restorative materials, whereas a hard and fast bite would yield a higher strain rate applied to the restorative materials. Based on the information provided by Fig. 7, the elastic properties of materials remain constant regardless the type of biting action.

3.3. *Fracture surface analysis*

Figs. 8 and 9 show the scanning electron micrographs of the fracture surfaces of the monolithic materials and composites after shear and flexural tests, respectively. The fractography analyses confirmed a good bonding between the metallic particles and the porcelain, with significant amount of metallic particles being retained in the ceramic rich composites after shear and flexural tests.

The fractographs of 20 M and 40 M composites after shear tests (Fig. 8) reveals metallic particles retained in the

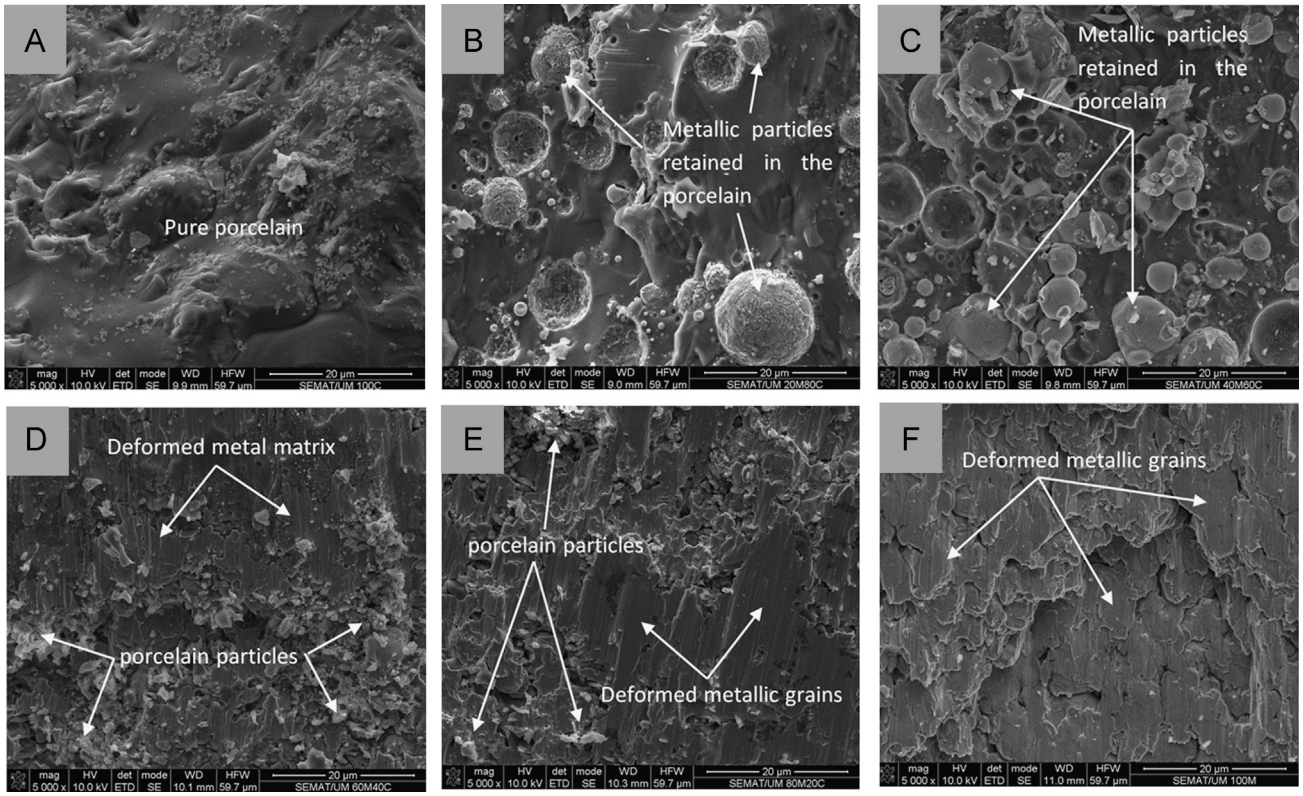

Fig. 8 – Micrographs showing the fracture surfaces of monolithic materials (A – 0 M and F – 100 M) and composite materials (B – 20 M; C – 40 M; D – 60 M; and E – 80 M) after shear tests.

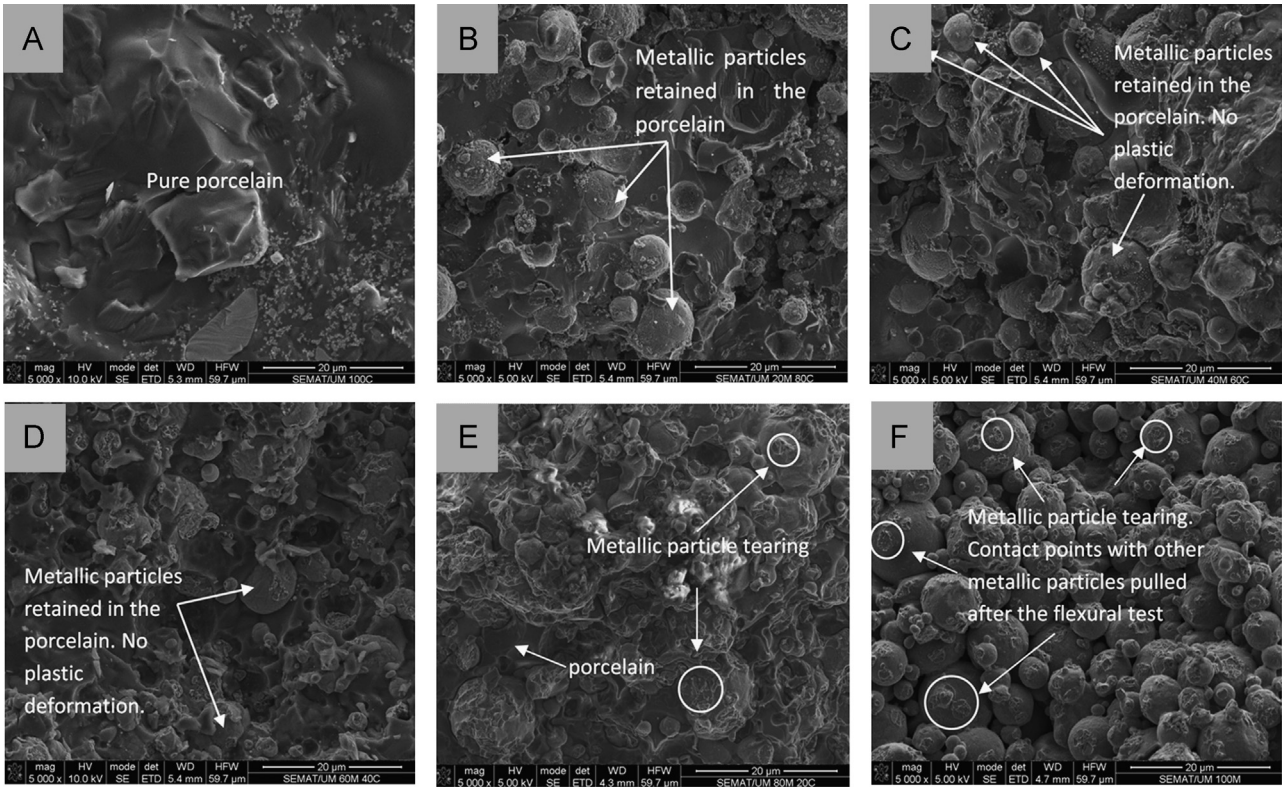

Fig. 9 – Micrographs showing the fracture surfaces of monolithic materials (A – 0 M and F – 100 M) and composite materials (B – 20 M; C – 40 M; D – 60 M; and E – 80 M) after flexural tests.

porcelain. The presence of metallic particles in these MMCs introduced significant toughness to the material as demonstrated in Fig. 5. The toughness mechanism can be explained by the presence of the metallic phase, which blunts the crack path and forces the crack to grow around the metallic particle (Agrawal and Sun, 2004). The partial debonding of the reinforcing particles during the test could also have accounted for a fracture toughness increase due to the higher volume of free material to be deformed plastically (Dlouhy and Boccaccini, 1996).

The composites 60 M and 80 M as well as the monolithic 100 M, exhibited extensive plastic deformation of the metallic phase during shear test (Fig. 8). Fragments of porcelain can also be seen in Fig. 8 in the fracture surfaces of 60 M and 80 M (Fig. 8D and E). Attending to the strength results, no strain hardening effect promoted by the porcelain phase could be observed.

The fractographs of samples subjected to flexural tests (Fig. 9) are similar to those described previously for shear tests, except the fact that no plastic deformation of the metallic phase could be observed in latter case. It can be explained by the fact that failure in flexural tests occurs mainly due to tensile stresses, conversely to what happens in shear test. It is interesting to note in 80 M and 100 M composites (Fig. 9E and F) the metallic particles tears present in the contact points of metallic particles with other particles that had been pulled out after flexural test. These finding confirms the early sintering stage indicated previously for the 100 M samples, corresponding to a stage where the necks are being formed (German, 1996). This fact is also important to understand the lower Young's modulus and the lack of ductility exhibited by the 100 M sample (hot pressed during 10 min). Moreover, the tears found in the metallic particles in 80 M composite gives further evidence that this composite was as a co-continuous composite, displaying an interconnecting network of metal phase (Agrawal and Sun, 2004).

4. Conclusions

The thermal, elastic and inelastic properties of CoCrMo–porcelain composites were studied. Within the limitations of this studied, the following conclusions can be drawn:

- CoCrMo particles exhibited good adhesion to the porcelain matrix.
- The incorporation of metallic particles in the ceramic matrix showed to increase the fracture strength (shear and flexural) of the composite.
- The presence of porcelain (ceramic phase) in the CoCrMo matrix showed to decrease the fracture strength (shear and flexural) of the composite.
- The monolithic materials (homogeneous porcelain and CoCrMo alloy) and composite materials (20–80 M) exhibited elastic modulus with frequency-independent behavior.
- The coefficient of thermal expansion (CTE) of metal–ceramic composites increases and hardness decreases

with increasing metallic particles content, but this increase is not linearly proportional to the composition.

Acknowledgments

The authors ackowledge the Portuguese Foundation for Science and Technology (FCT) and CAPES for the financial support. Assistance by M.Sc. M. Friman (Aalto Univeristy Foundation) in DMA and DIL experiments is also acknowledged.

REFERENCES

Agrawal, P., Sun, C.T., 2004. Fracture in metal–ceramic composites. Compos. Sci. Technol. 64, 1167–1178.

Anusavice, K.J., Horner, J.A., Fairhurst, C.W., 1977a. Adherence controlling elements in ceramic–metal systems. I. Precious alloys. J. Dent. Res. 56, 1045.

Anusavice, K.J., Horner, J.A., Fairhurst, C.W., 1977b. Adherence controlling elements in ceramic–metal systems. II. Nonprecious alloys. J. Dent. Res. 56, 1053.

Anusavice, K.J., 2012. Standardizing failure, success, and survival decisions in clinical studies of ceramic and metal–ceramic fixed dental prostheses. Dent. Mater. 28, 102–111.

Bieniaś, J., Surowska, B., Stoch, A., Matraszek, H., Walczak, M., 2009. The influence of SiO_2 and SiO_2–TiO_2 intermediate coatings on bond strength of titanium and Ti–6Al–4V alloy to dental porcelain. Dent. Mater. 25, 1128–1135.

Carrado, A., Palkowski, H., 2010. Microstructural and mechanical investigations on porcelain-fused-to-metal in multilayer system. Adv. Eng. Mater. 12 (4), b122–b127.

Dlouhy, I., Boccaccini, A.R., 1996. Preparation, microstructure and mechanical properties of metal-particulate/glass-matrix composites. Compos. Sci. Technol. 56, 1415–1424.

Elsaka, S.E., Hamouda, I.M., Elewady, Y.A., Abouelatta, O.B., Swain, M.V., 2010. Influence of chromium interlayer on the adhesion of porcelain to machined titanium as determined by the strain energy release rate. J. Dent. 38 (8), 648–654.

Gasik, M., 1998. Micromechanical modeling of functionally graded materials. Comput. Mater. Sci. 13, 42–55.

German, R.M., 1996. Sintering Theory and Practice. Wiley-Interscience, New York.

Hautaniemi, J.A., 1995. The effect of indium on porcelain bonding between porcelain and Au–Pd–In alloy. J. Mater. Sci.: Mater. Med. 6, 46–50.

Henriques, B., Soares, D., Silva, F., 2011. Optimization of bond strength between gold alloy and porcelain through a composite interlayer obtained by powder metallurgy. Mater. Sci. Eng. A 528, 1415–1420.

Henriques, B., Gasik, M., Soares, D., Silva, F., 2012a. Experimental evaluation of the bond strength between a CoCrMo dental alloy and porcelain through a composite metal–ceramic graded transition interlayer. J. Mech. Behav. Biomed. Mater. 13, 206–214.

Henriques, B., Felix, S., Soares, D., Silva, F., 2012b. Shear bond strength comparison between conventional porcelain fused to metal and new functionally graded dental restorations after thermal–mechanical cycling. J. Mech. Behav. Biomed. Mater. 13, 194–205.

Henriques, B., Soares, D., Silva, F., 2012c. Microstructure, hardness, corrosion resistance and porcelain shear bond strength comparison between cast and hot pressed CoCrMo alloy for metal–ceramic dental restorations. J. Mech. Behav. Biomed. Mater. 12, 83–92.

Henriques, B., Soares, D., Silva, F., 2012d. Influence of preoxidation cycle on the bond strength of CoCrMo–porcelain dental composites. Mater. Sci. Eng. C 32 (8), 2374–2380.

Henriques, B., Soares, D., Silva, F., 2013. Hot pressing effect on the bond strength of a CoCrMoSi alloy to a dental porcelain. Mater. Sci. Eng. C 33 (1), 557–563.

Maira, L., Padipatvuthikulb, P., 2010. Variables related to materials and preparing for bond strength testing irrespective of the test protocol. Dent. Mater. 26, e17–e23.

Oksiuta, Z., Dabrowskia, J.R., Olszynab, A., 2009. Co–Cr–Mo-based composite reinforced with bioactive glass. J. Mater. Process. Technol. 209, 978–985.

Özcan, M., 2003. Fracture reasons in ceramic-fused-to metal restorations. J. Oral Rehabil. 30, 265–269.

Özcan, I., Uysal, H., 2005. Effects of silicon coating on bond strength of two different titanium ceramic to titanium. Dent. Mater. 21, 773–779.

Suresh, S., 2001. Graded materials for resistance to contact deformation and damage. Science 292, 2447–2451.

Swain, M.V., 2009. Unstable cracking (chipping) of veneering porcelain on all-ceramic dental crowns and fixed partial dentures. Acta Biomater. 5, 1668–1677.

Wagner, W.C., Asgar, K., Bigelow, W.C., Flinn, R.A., 1993. Effect of interfacial variables on metal–porcelain bonding. J. Biomed. Mater. Res. 27, 531–537.

Yesil, Z.D., Karaoglanoglu, S., Akyıl, M.S., Seven, N., 2009. Evaluation of the bond strength of different bonding agents to porcelain and metal alloy. Int. J. Adhes. Adhes. 29, 32–35.

Zhang, Y., Kim, J.W., 2009. Graded structures for damage resistant and aesthetic all-ceramic restorations. Dent. Mater. 25, 781–790.